EUROPEAN

NETWORK

MAX-PLANCK-GESELLSCHAFT

The accretion process in the nucleus of the radio galaxy PKS 1333−33

T. Venturi[1]⋆, S. Pellegrini[2], A. Comastri[3], R. Morganti[4]⋆, and C. Vignali[5]

[1] Istituto di Radioastronomia, CNR, Via Gobetti 101, Bologna, Italy
[2] Dipartimento Astronomico, Università di Bologna, via Ranzani 1, 40126 Bologna, Italy
[3] Osservatorio Astronomico, Via Ranzani 1, 40126 Bologna, Italy
[4] NFRA, Postbus 2, AA 7990 Dwingeloo, The Netherlands
[5] Dept. of Astronomy and Astrophysics, Penn State Univ., 525 Davey Lab, University Park, PA 16802, USA

Abstract. We present multi-frequency radio observations at parsec–scale resolution of the elliptical galaxy IC4296. The associated radio galaxy, PKS 1333−33, is intermediate between FRI and FRII, with very extended radio jets, slightly asymmetric in brightness, and faint hot spots. ASCA and BeppoSAX X–ray observations of IC4296 showed an excess of hard emission with respect to the expected stellar contribution, suggesting the presence of a low luminosity AGN or an obscured nucleus. Recent Chandra observations have been able to reveal for the first time a bright (although partially absorbed) nucleus. The parsec–scale radio images and spectral properties support the idea that the radio core is active and efficient in feeding the large scale radio jets, while the observed X–ray nuclear properties (especially the low 2–10 keV luminosity level) are still to be explained. We use a Hubble constant $H_0 = 50$ km s^{-1}Mpc^{-1}, which implies 1 mas = 0.35 pc at the distance of PKS 1333−33. We assume $S \propto \nu^{-\alpha}$.

1. Broad band properties of PKS 1333−33

PKS 1333−33 is a classical nearby (z=0.012465) double radio source, associated with the elliptical galaxy IC 4296, the dominant member of the cluster of galaxies A3565.

Radio images over a wide range of frequencies and angular scales show two jets, aligned in position angle $\sim 130°$, culminating in two lobes (Killeen et al. 1986). The north–western arcsecond jet is slightly brighter, and points towards the strongest lobe, which contains also a high brightness peak, similar to a hot spot. The morphology and total power of this source, $\log P_{5\,\text{GHz}}$ (W Hz^{-1})=24.7, are consistent with the idea that it is intermediate between FRI and FRII radio galaxies (Fanaroff & Riley 1974).

The optical spectrum is dominated by a stellar continuum, as typical for early–type galaxies, with weak lines and no signature of strong nuclear activity (Tadhunter et al. 1998). No HI absorption was detected on the arc–second scale (Morganti et al. 2001).

ASCA and BeppoSAX X–ray spectra show a hard X–ray excess over the predicted contribution from stellar sources (Sambruna et al. 1999), interpreted to be of nuclear origin. Its L_X luminosity (in the 2–10 keV band) is of the order of a few times 10^{41} erg s^{-1}, a value orders of magnitude lower than the expected Eddington luminosity, if we assume a central black hole mass of $M_{\text{BH}} \sim 7.5 \times 10^8$ $M_\odot$ (as derived on the basis of the bulge mass – black hole mass relation, Kormendy & Richstone 1995). This inconsistency can be explained either assuming an advection dominated accretion flow (ADAF, Narayan & Yi 1995), or by strong absorption of the X–ray luminosity

from Compton thick material surrounding the active nucleus.

ADAF models predict that the spectrum of the radio nucleus is self–absorbed up to the cm–mm regime, with a dramatic steepening after the turnover (e.g. Di Matteo, Carilli & Fabian 2001). VLBI radio observations are therefore an important tool to test this model. The observations presented here are expected to make an important contribution to shedding light on the accretion mechanism at the centre of PKS 1333−33.

2. The radio observations and images

PKS 1333−33 was observed at 8.4 GHz, 15 GHz and 22 GHz with the Very Long Baseline Array[1] , including also one VLA antenna. We cycled among these three frequencies during the 5 hours of the source visibility, for a total time on source of about 1.5 hr per frequency. The data reduction and image analysis were carried out with the AIPS package. We note that fringes were found only in the baseline range $\sim 0-80$ Mλ at each frequency; therefore only a limited array (7 antennas) was used for self–calibration and imaging. Details of the observations and images are given in Table 1.

The 8.4 GHz image of PKS 1333−33 is presented in Figure 1. It is characterised by an asymmetric double morphology, with a compact nuclear component and two short jets. The parsec–scale core contains $\sim$90% of the total flux density, and two jets are aligned in position angle (P.A.)

---

[1] The VLBA from the National Radio Astronomy Observatory is operated by Associated Universities, Inc. under a Cooperative Agreement with the National Science Foundation.

Table 1. Observational Details

ν GHz	$FWHM^{a}$ mas, P.A.	rms mJy/b	S_p mJy/b	S_{tot} mJy
8.4	$5.0 \times 2.0, 45°$	0.068	135.1	173.5
15.4	$5.2 \times 1.3, -6°$	0.25	60.8	174.0
22.2	$5.0 \times 2.0, 45°$	1.4	154.2	157.9

[a] The FWHM given refers to the final image.
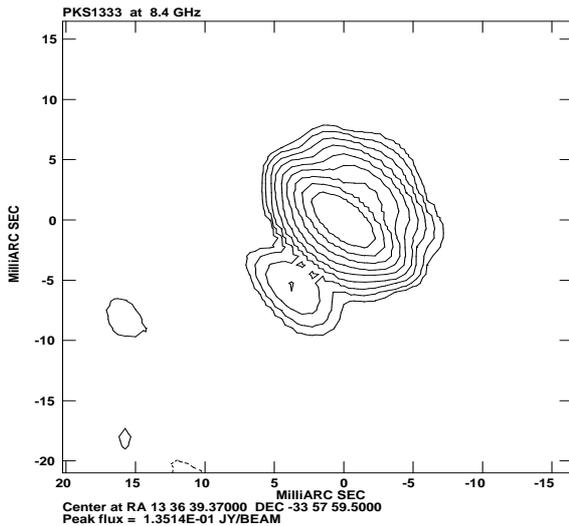
Fig. 1. 8.4 GHz VLBA image of PKS 1333−33. The resolution is 5×2 mas, P.A. 0°. Logarithmic contours are given, the lowest being 0.2 mJy/b. The root-mean-square (rms) noise in the image is 68μJy.

$\sim 140°$, in fairly good agreement with the orientation of the large scale jets. The jet–to–counterjet peak brightness asymmetry is ~ 8, i.e. $\beta \cos \theta \sim 0.39$. This leads to a limit on the viewing angle $\theta_{\max} \sim 66°$, in agreement with the estimate obtained on the basis of the core dominance (Venturi et al. 2000). We note that the brightest jet in this image is aligned with the brightest arc–second scale one.

The 15 GHz and 22 GHz images, not shown here, are only barely resolved, and no parsec–scale jet emission was detected with the resolution and sensitivity of our images.

3. Comments on the nuclear radio spectrum

We used the values given in Table 1, together with literature results, to derive the radio spectrum of the arcsec and mas core of PKS 1333−33, shown in Figure 2, in order to test its consistency with the expectations from the ADAF model. The arcsec core flux density at 2.3 GHz is from Morganti et al. (1997), those at 1.4, 5, 15 and 22 GHz are from Killeen et al. (1986). The VLBI 2.3 GHz flux density is from Venturi et al. (2000).

The arcsec core spectrum peaks at ~ 15 GHz, and steepens dramatically beyond the turnover, similarly to the results found by Di Matteo, Carilli & Fabian (2001) for a few sources selected to test a set of ADAF models. The
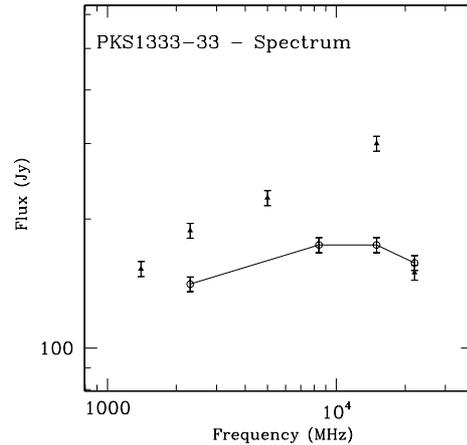
Fig. 2. Radio spectrum of the nucleus in PKS 1333−33. Filled triangles refer to the arcsecond nucleus, open circles to the parsec–scale one.

spectral index is $\alpha \sim -0.3$ for $\nu < 15$ GHz and $\alpha \sim 1.8$ for $\nu > 15$ GHz. The spectrum of the parsec–scale core is still convex, but less extreme values for the spectral index are found. In particular, $\alpha \sim -0.16$ in the range 2.3 GHz $< \nu <$ 8.4 GHz, $\alpha \sim 0.25$ for $\nu > 15$ GHz.

We note that the difference between the arcsec and mas core flux density in PKS 1333−33 steadily increases from 2.3 GHz to 15 GHz. In particular, we have S_{mas}/S_{asec}=75% at 2.3 GHz, and S_{mas}/S_{asec}=58% at 15 GHz. The very different epochs of the observations (there is a gap longer than 15 years between Killeen's and ours) might account for part of the difference, assuming that some variability exists in the source. However, these percentages suggest the existence of extended flux density on the parsec–scale, undetected by our observations (due to low brightness and/or spatial frequencies undetectable with our u–v coverage).

A detailed discussion on the accretion process in PKS 1333−33 will be given in a forthcoming paper, where our VLBI results will be analysed together with almost simultaneous Chandra X–ray images (Pellegrini et al. in preparation).

References

Di Matteo, T., Carilli, C.L. & Fabian, A.C., 2001, ApJ, 547, 731
Fanaroff, B.L. & Riley, J.M., 1974, MNRAS, 167, 31
Killeen, N., Bicknell, G.V. & Ekers, R.D., 1986, ApJ, 302, 306
Kormendy, J. & Richstone, D., 1995, ARA&A, 33, 581
Morganti, R., Oosterloo, T.A., Reynolds, J.E., et al., 1997, MNRAS, 284,541
Morganti, R., Oosterloo, T.A., Tadhunter, C.N., et al., 2001, MNRAS, 323, 331
Narayan, R., Yi, I., 1995, ApJ, 452, 710
Sambruna, R.M., Eracleous, M. & Mushotzky, R.F., 1999, ApJ, 526, 60
Tadhunter, C.N., Morganti R., Robinson, A., et al., 1998, MNRAS, 298, 1035
Venturi, T., Morganti, R., Tzioumis, T., et al., 2000, A&A, 363, 84